

This discussion paper is/has been under review for the journal Atmospheric Chemistry and Physics (ACP). Please refer to the corresponding final paper in ACP if available.

Microwave Limb Sounder observations of biomass-burning products from the Australian bush fires of February 2009

H. C. Pumphrey¹, M. L. Santee², N. J. Livesey², M. J. Schwartz², and W. G. Read²

¹School of GeoSciences, The University of Edinburgh, Edinburgh, UK

²NASA Jet Propulsion Laboratory, Pasadena, CA, USA

Received: 14 January 2011 – Accepted: 11 February 2011 – Published: 23 February 2011

Correspondence to: H. C. Pumphrey (h.c.pumphrey@ed.ac.uk)

Published by Copernicus Publications on behalf of the European Geosciences Union.

MLS observations of burning products

H. C. Pumphrey et al.

Title Page

Abstract

Introduction

Conclusions

References

Tables

Figures

◀

▶

◀

▶

Back

Close

Full Screen / Esc

Printer-friendly Version

Interactive Discussion



Abstract

The large bush fires which occurred in southeast Australia in February 2009 were unusually destructive. However, they were also unusual in the amounts of various combustion products which were injected directly into the stratosphere. We report the observations by the Microwave Limb Sounder (MLS) instrument on the Aura satellite of some of these combustion products. The highest quality observations are of CO; these clearly show a large region of enhanced mixing ratios to the north of New Zealand which remains in that region for about ten days before drifting westwards and finally dissipating over the Atlantic about a month after the fire. Back trajectories run from the points where MLS observes enhanced CO pass close to the site of the fire. The MLS observations of CH₃CN and HCN resemble those of CO except for their poorer vertical resolution and more limited vertical range. An apparent enhancement in ClO is also observed by MLS, but detailed analysis of the measured radiances reveals this feature to be a signature of CH₃OH, which is not currently retrieved by the MLS data processing system. The fires of February 2009 are the only event of this type and magnitude in the 6-yr MLS record.

1 Introduction

On 7 February 2009, the state of Victoria suffered the most damaging series of bush fires on record for Australia. 173 lives were lost and the damage has been estimated by a Royal Commission (Teague et al., 2010) to be of the order of AUS\$4.4 billion. The event has become known as Black Saturday. One of the many extreme aspects of this event was the altitude reached by the plume of combustion products. These products include both smoke particles and gases. In this paper we report on the gaseous combustion products as observed by the Microwave Limb Sounder (MLS) instrument on NASA's Aura platform.

ACPD

11, 6531–6554, 2011

MLS observations of burning products

H. C. Pumphrey et al.

Title Page

Abstract

Introduction

Conclusions

References

Tables

Figures

◀

▶

◀

▶

Back

Close

Full Screen / Esc

Printer-friendly Version

Interactive Discussion



**MLS observations of
burning products**

H. C. Pumphrey et al.

Aura (Schoeberl et al., 2006) was launched in July 2004, and the MLS instrument (Waters et al., 2006) has operated almost flawlessly from August 2004 to date. MLS measures the mixing ratios of a number of chemical species, including several biomass burning products. It was known prior to the MLS launch that injections of such gases into the lower stratosphere do occur (see e.g. Fromm and Servranckx, 2003; Fromm et al., 2010), and can be observed by a microwave limb-sounding instrument (Livesey et al., 2004). It was part of the MLS science plan to observe any such events that might occur during the mission: the Black Saturday fires were the first such event.

2 The observations

MLS consists of a 2 m parabolic dish antenna feeding heterodyne radiometers operating at 118, 190, 240 and 640 GHz. A separate small antenna feeds another radiometer operating at 2.5 THz. The output of the radiometers is analysed by banks of filters. The antenna looks forward from the Aura platform, in the plane of the orbit, and is scanned across the Earth's limb 240 times per orbit. As the orbit is inclined at 98° to the equator, the instrument observes a latitude range from 82° S to 82° N every day. The radiation observed is emitted thermally by the atmosphere, so observations can be made day and night. The orbit is sun-synchronous, so the observations are always made at the same two local times for a given latitude. The radiances reported by the filter banks are used as input to a software package (Livesey et al., 2006) which estimates profiles of temperature, and of the mixing ratios of the target chemical species. All mixing ratios in this paper are produced by version 2.2 (V2.2) of this software package.

Among the suite of MLS V2.2 measurements are three biomass-burning products: CO (Livesey et al., 2008; Pumphrey et al., 2007), HCN (Pumphrey et al., 2006, 2008) and CH₃CN. Of these, the CO data are the most reliable and best-validated. MLS data are reported on pressure levels spaced at 6 levels per pressure decade (a spacing of approximately 2.7 km). The CO data are of good quality at the 100 hPa and 147 hPa levels and at all higher altitudes in the middle atmosphere. At the 215 hPa

[Title Page](#)[Abstract](#)[Introduction](#)[Conclusions](#)[References](#)[Tables](#)[Figures](#)[◀](#)[▶](#)[◀](#)[▶](#)[Back](#)[Close](#)[Full Screen / Esc](#)[Printer-friendly Version](#)[Interactive Discussion](#)

level the data are usable with care: a positive bias of about 100% must be accounted for (Livesey et al., 2008). The HCN and CH₃CN data have not been extensively validated (Livesey et al., 2007). The HCN data are known to have large biases in the lower stratosphere (100 hPa–10 hPa). Two separate CH₃CN products are produced: one from the 190 GHz region and one from the 640 GHz region; both products have obvious problems and must be used with some caution. Although the 190 GHz CH₃CN was the standard product in V2.2, subsequent analysis suggests that the 640 GHz CH₃CN is more realistic; it will become the standard CH₃CN product in subsequent versions of the data. As the CO is the most reliable of these three MLS measurements of biomass-burning products, we used it to obtain an overview of the Black Saturday event.

2.1 Mapping the plume

Figure 1 shows the MLS CO mixing ratio at 100 hPa on 12 and 13 February 2009. The orbits from 13 February lie in between the orbits from 12 February.

As we will show later, the region of large values to the north of New Zealand is a direct result of the Black Saturday fires. Figure 1 is typical of the two weeks following the fire. To summarise the development of the fire-affected airmass, we began by identifying which of the MLS measurements are clearly part of that airmass. We did this by finding the mean value and standard deviation for all measurements in a given latitude band and at a given pressure level. We then defined a point as affected if its mixing ratio was more than 4.2 standard deviations above the mean. (The value of 4.2 is somewhat arbitrary but in practice tends to detect most of the interesting events while rejecting almost all of the background points.) An iterative approach is used to ensure that the mean and standard deviation are calculated from the unaffected points; there are few enough affected points that this calculation converges very quickly. Figure 2 shows the locations of the affected points in four consecutive 6-day periods. The points are clustered to the north of New Zealand and to the east of Australia for the first six days. In the next six days the plume of pollutants becomes elongated and drawn

MLS observations of burning products

H. C. Pumphrey et al.

Title Page

Abstract

Introduction

Conclusions

References

Tables

Figures

◀

▶

◀

▶

Back

Close

Full Screen / Esc

Printer-friendly Version

Interactive Discussion



out towards the southeast. Over the following twelve days most of the plume moves northwestwards and then westwards, passing across the Indian ocean towards Africa. A smaller component at 100 hPa moves towards the southeast; this is just visible in the third panel of Fig. 2.

To further summarise the history of the polluted airmass, we show in Fig. 3 the number of points identified as unusual at each MLS pressure level, as a function of time. Figure 4 shows how many standard deviations above the mean the points identified as unusual in Fig. 3 were. It is clear from Figs. 3–4 that the event is observable from day 39 of 2009 (8 February), the day after the fires, until day 70 of 2009 (11 March). It is also clear from Figs. 2–4 that the 46 hPa level is not affected by the plume until the 8th day of the event, and remains affected after the other levels have returned to their background values. This suggests that the polluted region is ascending as it moves.

2.2 Enhancements of other species in the polluted airmass

2.2.1 Retrieved mixing ratios

The large enhancement in CO is the most obvious difference between the polluted airmass described above and the surrounding air. We now consider whether any of the other species observed by MLS are enhanced or depleted within the polluted airmass. An MLS measurement location was marked as being polluted by using the CO mixing ratio as described in Sect. 2.1, and the daily mean mixing ratio of various species for the marked locations was calculated. Where there are no affected points we show an average from whichever three points happened to have the largest CO mixing ratio. Some results are shown in Figs. 5 and 6; CO itself is plotted in Fig. 5 to facilitate direct comparison. Similar plots (not shown) were made for H₂O, HNO₃, SO₂, HCl and O₃, none of which showed any obvious difference between the polluted period and the periods before and after.

HCN and CH₃CN both have biomass burning as their only significant source in the atmosphere (Singh et al., 2003; Li et al., 2003). HCN, together with CO, has been

MLS observations of burning products

H. C. Pumphrey et al.

Title Page

Abstract

Introduction

Conclusions

References

Tables

Figures



Back

Close

Full Screen / Esc

Printer-friendly Version

Interactive Discussion



**MLS observations of
burning products**

H. C. Pumphrey et al.

[Title Page](#)[Abstract](#)[Introduction](#)[Conclusions](#)[References](#)[Tables](#)[Figures](#)[◀](#)[▶](#)[◀](#)[▶](#)[Back](#)[Close](#)[Full Screen / Esc](#)[Printer-friendly Version](#)[Interactive Discussion](#)

previously observed from space to have elevated values in regions affected by biomass burning (Rinsland et al., 2005, 2007). The MLS HCN product is not recommended for general use in the 100 hPa–10 hPa range as it has large biases. It can, however, be used to qualitatively indicate large changes in the HCN mixing ratio. Retrieval of HCN is not attempted at pressures greater than 100 hPa. At the levels where it is retrieved, HCN shows enhancements at similar times and altitudes to those shown by CO.

MLS is sensitive to CH₃CN in two of its radiometers: those at 190 GHz and 640 GHz. The retrieval software produces two separate CH₃CN products but the 190 GHz product is not of usable quality, so we show only the 640 GHz product in Fig. 5. As with HCN, this shows a significant increase at similar times and altitudes to those shown by CO.

Chlorine monoxide (ClO) is not normally thought of as a product of biomass burning. As with CH₃CN, MLS measures ClO in both the 640 GHz and 190 GHz radiometers. Unlike CH₃CN, both ClO products are considered to be useful. The 640 GHz product is of higher quality (Santee et al., 2008) and is the standard product recommended for general use. The 640 GHz product shows a substantial enhancement in the polluted airmass, but the 190 GHz product shows no enhancement at all (Fig. 6). This suggests that there are unusual amounts of some molecule in the plume which is not ClO and which has spectral lines in the 640 GHz ClO band, but not in the 190 GHz ClO band. It is suggested by Santee et al. (2008) that the most likely candidate molecules are methyl chloride (chloromethane: CH₃Cl) and methanol (CH₃OH). We investigate these possibilities by examining the measured radiances.

2.2.2 Radiances

We examined the radiances in the plume by choosing a day (14 February) on which the measurements with enhanced CO are located in a particularly small region: 30°–35° S, 160°–180° W. We averaged the radiances from limb scans which lie within that region. We then subtracted radiances for the same latitudes and all other longitudes from this mean. The spectral features which show up should therefore be due to the pollution

and not to latitudinal gradients. We show the results for the 190 GHz radiometer in Fig. 7 and for the 640 GHz radiometer in Fig. 8. As an aid to interpretation we also show in Figs. 7 and 8 some calculated spectral differences. These were produced by using a radiative transfer model to calculate the radiances which MLS would observe for a typical atmosphere, and then for the same atmosphere with the mixing ratio of a single species enhanced at the 100 and 68 hPa levels. If the measured radiance differences in the top panel show features similar to the calculated differences in one of the other panels, this implies that the species which is enhanced in the calculation for the lower panel was also enhanced in the plume region.

The 190 GHz radiances from the plume are clearly enhanced in bands 6 and 27 due to HCN. The enhancement in bands 2 and 4 due to CH_3CN is less clear against a more spectrally flat enhancement. This latter effect is probably due to water vapour: the plume is considerably wetter than the latitudinal average although not to a statistically unusual extent due to the high variability of water vapour. There is no clear enhancement in the centre of band 5 of the instrument; this explains why the ClO retrieved from this band also shows no enhancement.

The top panel of Fig. 8 shows that the 640 GHz radiances from the plume region are clearly enhanced in bands 14, 30 and 31; comparison with the third panel suggests that this enhancement is consistent with an enhanced CH_3CN mixing ratio. The radiances from the plume are also clearly enhanced in bands 10, 11, 28 and 29. The enhancement is strongest in the centre of band 10. Comparison with the lower four panels of Fig. 8 suggests that this enhancement would not be consistent with enhancement of CH_3Cl alone, but would be consistent with an enhancement of either methanol or ClO. However, we know from the 190 GHz radiances that the enhancement in ClO is negligible, leaving methanol as the most likely candidate. Note that some CH_3Cl may also be present in the plume; it is difficult to be certain about this but the asymmetric shape of the spectral peak is suggestive.

The calculated spectral radiance differences in the second panel of Fig. 8 were generated by increasing the methanol mixing ratio by 9.2 ppbv at 68 hPa and 3 ppbv at

MLS observations of burning products

H. C. Pumphrey et al.

Title Page

Abstract

Introduction

Conclusions

References

Tables

Figures

◀

▶

◀

▶

Back

Close

Full Screen / Esc

Printer-friendly Version

Interactive Discussion



100 hPa. We next ask if an enhancement of that magnitude is likely, given the mixing ratio increase of CO. On 14 February, the CO values in the plume were about 180 ppbv and 220 ppbv above the background value at 100 hPa and 68 hPa, respectively. This implies a CH₃OH/CO emission ratio between 0.017 and 0.042 in reasonable agreement with the values in the literature. These range from 0.006 to 0.037 (Christian et al., 2003) with many reported values being close to 0.018 (Paton-Walsh et al., 2008; Andreae and Merlet, 2001). An earlier measurement of both CO and CH₃OH from space (Rinsland et al., 2007) gives an emission ratio of 0.0278 ± 0.00456 . The agreement of the methanol emission ratios estimated from the MLS measurements of the Black Saturday plume with those in the literature supports our hypothesis that methanol is the main species responsible for the signal observed in the 640 Gz radiometer of MLS.

3 Attribution

While it seems a reasonable working hypothesis that the polluted air mass observed by MLS is the result of the Black Saturday fires, the observations for the first 12 days of the event are clustered in a rather restricted region which is not located over Victoria, but to the north of New Zealand. In order to strengthen or refute the hypothesis, we ran back-trajectory calculations from the MLS observations. The trajectories were produced using the online trajectory service of the British Atmospheric Data Centre (BADC) (<http://badc.nerc.ac.uk/community/trajectory>) driven by winds from the operational analysis of the European Centre for Medium-range Weather Forecasting (ECMWF). Trajectories were launched at the latitude, longitude and pressure of each of the MLS positions where the CO mixing ratio was identified as unusually high. If there were anomalous CO values at two adjacent pressure levels, an extra trajectory was launched at an intermediate pressure as well. Two examples are shown in Fig. 9. Back trajectories like those in Fig. 9 were run for every hour in which an MLS observation of elevated CO was made during the ten days after the fires. The results are summarised in Fig. 10. These trajectory calculations show that most of the polluted air parcels moved past

MLS observations of burning products

H. C. Pumphrey et al.

Title Page

Abstract

Introduction

Conclusions

References

Tables

Figures

◀

▶

◀

▶

Back

Close

Full Screen / Esc

Printer-friendly Version

Interactive Discussion



southeastern Australia, travelling in an east-southeastwards direction, on the day of the fire. They reached New Zealand within a day and spent at least the next eight days executing anti-cyclonic motion in the region to the north of New Zealand. The process which injected the pollution into the stratosphere occurs on far too small a spatial scale to be captured by the trajectory calculations. However, the clustering of the closest passes to the south of the coast suggests that processes in the troposphere transported the pollutants south and west from the fire during the course of the injection process.

4 The wider context

In order to gain some understanding as to how unusual the Black Saturday event was for the lower stratosphere, we repeat the analysis shown in Figs. 3 and 4 for the entire MLS mission to date. The results are shown in Fig. 11. Viewed in terms of number of MLS locations affected per day, the Black Saturday event does not look unusual at a first glance. However, the most conspicuous feature is the annual biomass-burning season in South America and southern Africa. This occurs in the second half of the year and affects mostly the 316–100 hPa altitude range. The Black Saturday event affects the 100–46 hPa range and occurs in the first part of the calendar year. When viewed in terms of the extent to which the affected airmass differs from the usual behaviour of the atmosphere, the Black Saturday event very clearly stands out from any other event in the record. We carried out similar calculations to those shown in Fig. 11 for the other latitude regions of the Earth; again, we found no events in any way similar to the Black Saturday event.

The plume from the Black Saturday event has been observed by instruments other than MLS, including CALIPSO (Winker et al., 2010), Odin-OSIRIS (Siddaway and Petelina, 2011) and MIPAS on Envisat (Sembhi, 2011). The position and motion of the plume observed by these instruments is in agreement with that observed by MLS.

MLS observations of burning products

H. C. Pumphrey et al.

Title Page

Abstract

Introduction

Conclusions

References

Tables

Figures



Back

Close

Full Screen / Esc

Printer-friendly Version

Interactive Discussion



5 Conclusions

In February/March 2009 MLS observed an unusual airmass in the lower stratosphere containing high concentrations of several biomass-burning products. Biomass-burning products directly observed by MLS in this airmass are CO, HCN, CH₃CN, CH₃OH and possibly CH₃Cl. The ClO mixing ratios retrieved from the 640 GHz MLS data imply that the airmass has enhanced ClO mixing ratios. This is, however, almost certainly due to CH₃OH, which has a similar spectral signature to ClO in the spectral region covered by MLS band 10. Trajectory calculations link this polluted airmass to the large bush fires which occurred in the state of Victoria, Australia on 7 February 2009. There is no other event of the same type and magnitude in the Aura MLS dataset.

Acknowledgements. Work at the Jet Propulsion Laboratory, California Institute of Technology, was carried out under a contract with the National Aeronautics and Space Administration. HCP thanks the University of Edinburgh for granting the sabbatical time during which this paper was written. Thanks are also due to Svetlana Petelina and Harjinder Sembhi for various helpful suggestions.

References

- Andreae, M. O. and Merlet, P.: Emission of trace gases and aerosols from biomass burning, *Global Biogeochem. Cy.*, 15, 955–966, 2001. 6538
- Christian, T. J., Kleiss, B., Yokelson, R. Y., Holzinger, R., Crutzen, P. J., Hao, W. M., Saharjo, B. H., and Ward, D. E.: Comprehensive laboratory measurements of biomass-burning emissions: 1. Emissions from Indonesian, African and other fuels, *J. Geophys. Res.*, 108, 4719, doi:10.1029/2003JD003704, 2003. 6538
- Fromm, M. D. and Servranckx, R.: Transport of forest fire smoke above the tropopause by supercell convection, *Geophys. Res. Lett.*, 30, 1542, doi:10.1029/2002GL016820, 2003. 6533
- Fromm, M., Lindsey, D. T., Servranckx, R., Yue, G., Trickl, T., Sica, R., Doucet, P., and Godin-Beekmann, S.: The Untold Story of Pyrocumulonimbus, *Bull. Am. Meteorol. Soc.*, 91, 1193–1209, doi:10.1175/2010BAMS3004.1, 2010. 6533

ACPD

11, 6531–6554, 2011

MLS observations of burning products

H. C. Pumphrey et al.

Title Page

Abstract

Introduction

Conclusions

References

Tables

Figures

◀

▶

◀

▶

Back

Close

Full Screen / Esc

Printer-friendly Version

Interactive Discussion



**MLS observations of
burning products**

H. C. Pumphrey et al.

Title Page

Abstract

Introduction

Conclusions

References

Tables

Figures

◀

▶

◀

▶

Back

Close

Full Screen / Esc

Printer-friendly Version

Interactive Discussion



- Li, Q., Jacob, D. J., Yantosca, R. M., Heald, C. L., Singh, H. B., Koike, M., Zhao, Y., Sachse, G. W., and Streets, D. G.: A global three-dimensional model analysis of the atmospheric budgets of HCN and CH₃CN: Constraints from aircraft and ground measurements, *J. Geophys. Res.*, 108, 8827, doi:10.1029/2002JD003075, 2003. 6535
- 5 Livesey, N. J., Fromm, M. D., Waters, J. W., Manney, G. L., Santee, M. L., and Read, W. G.: Enhancements in lower stratospheric CH₃CN observed by UARS MLS following boreal forest fires., *J. Geophys. Res.*, 109, D06308, doi:10.1029/2003JD004055, 2004. 6533
- Livesey, N. J., Snyder, W. V., Read, W. G., and Wagner, P. A.: Retrieval algorithms for the EOS Microwave Limb Sounder (MLS) instrument, *IEEE T. Geosci. Remote Sens.*, 44, 1144–1155, 10 2006. 6533
- Livesey, N. J., Read, W. G., Lambert, A., Cofield, R. E., Cuddy, D. T., Froidevaux, L., Fuller, R. A., Jarnot, R. F., Jiang, J. H., Jiang, Y. B., Knosp, B. W., Kovalenko, L. J., Pickett, H. M., Pumphrey, H. C., Santee, M. L., Schwartz, M. J., Stek, P. C., Wagner, P. A., Waters, J. W., and Wu., D. L.: Earth Observing System (EOS) Aura Microwave Limb Sounder (MLS) Version 2.2 Level 2 data quality and description document., Tech. Rep. JPL D-33509, NASA Jet Propulsion Laboratory California Institute of Technology, Pasadena, California, 91109-8099, 15 http://mls.jpl.nasa.gov, 2007. 6534
- Livesey, N. J., Filipiak, M., Froidevaux, L., Read, W., Lambert, A., Santee, M., Jiang, J., Pumphrey, H., Waters, J., Cofield, R., Cuddy, D., Daffer, W., Drouin, B., Fuller, R., Jarnot, R., Jiang, Y., Knosp, B., Li, Q., Perun, V., Schwartz, M., Snyder, W., Stek, P., Thurstans, R., Wagner, P., Avery, M., Browell, E., Cammas, J.-P., Christensen, L., Diskin, G., Gao, R.-S., Jost, H.-J., Loewenstein, M., Lopez, J., Nedelec, P., Osterman, G., Sachse, G., and Webster, C.: Validation of Aura Microwave Limb Sounder O₃ and CO observations in the upper troposphere and lower stratosphere, *J. Geophys. Res.*, 113, D15S02, doi:10.1029/2007JD008805, 20 2008. 6533, 6534
- Paton-Walsh, C., Wilson, S. R., Jones, N. B., and Griffith, D. W. T.: Measurement of Methanol Emissions from Australian Wildfires by Ground-based Solar Fourier Transform Spectroscopy, *Geophys. Res. Lett.*, 35, L01880, doi:10.1029/2007GL032951, 2008. 6538
- Pumphrey, H. C., Jimenez, C. J., and Waters, J. W.: Measurement of HCN in the middle atmosphere by EOS MLS, *Geophys. Res. Lett.*, 33, L08804, doi:10.1029/2005GL025656, 2006. 6533
- 30 Pumphrey, H. C., Filipiak, M. J., Livesey, N. J., Schwartz, M. J., Boone, C., Walker, K. A., Bernath, P., Ricaud, P., Barret, B., Clerbaux, C., Jarnot, R. F., Kovalenko, L. J., Manney,

**MLS observations of
burning products**

H. C. Pumphrey et al.

Title Page

Abstract

Introduction

Conclusions

References

Tables

Figures

◀

▶

◀

▶

Back

Close

Full Screen / Esc

Printer-friendly Version

Interactive Discussion



- G. L., and Waters, J. W.: Validation of middle-atmosphere carbon monoxide retrievals from MLS on Aura, *J. Geophys. Res.*, 112, D24S38, doi:10.1029/2007JD008723, 2007. 6533
- Pumphrey, H. C., Boone, C., Walker, K. A., Bernath, P., and Livesey, N. J.: Tropical tape recorder observed in HCN, *Geophys. Res. Lett.*, 35, L05801, doi:10.1029/2007GL032137, 2008. 6533
- 5 Rinsland, C. P., Boone, G. D. C. D., Bernath, P. F., and Chiou, L.: Atmospheric Chemistry Experiment (ACE) measurements of elevated Southern Hemisphere upper tropospheric CO, C₂H₆, HCN, and C₂H₂ mixing ratios from biomass burning emissions and long-range transport, *Geophys. Res. Lett.*, 32, L20803, doi:10.1029/2005GL024214, 2005. 6536
- 10 Rinsland, C. P., Dufour, G., Boone, C. D., Bernath, P. F., Chiou, L., Pierre-Fran c. C., Turquety, S., and Clerbaux, C.: Satellite boreal measurements over Alaska and Canada during June–July 2004: Simultaneous measurements of upper tropospheric CO, C₂H₆, HCN, CH₃Cl, CH₄, C₂H₂, CH₃OH, HCOOH, OCS, and SF₆ mixing ratios, *Global Biogeochem. Cy.*, 21, GB3008, doi:10.1029/2006GB002795, 2007. 6536, 6538
- 15 Santee, M. L., Lambert, A., Read, W. G., Livesey, N. J., Manney, G. L., Cofield, R. E., Cuddy, D. T., Daffer, W. H., Drouin, B. J., Froidevaux, L., Fuller, R. A., Jarnot, R. F., Knosp, B. W., Perun, V. S., Snyder, W. V., Stek, P. C., Thurstans, R. P., Wagner, P. A., Waters, J. W., Connor, B., Urban, J., Murtagh, D., Ricaud, P., Barret, B., Kleinbohl, A., Kuttippurath, J., Kullmann, H., von Hobe, M., Toon, G. C., and Stachnik, R. A.: Validation of the Aura Microwave Limb Sounder ClO measurements, *J. Geophys. Res.*, 113, D15S22, doi:10.1029/2007JD008762, 2008. 6536
- 20 Schoeberl, M. R., Douglass, A. R., Hilsenrath, E., Bhartia, P. K., Barnett, J., Beer, R., Waters, J., Gunson, M., Froidevaux, L., Gille, J., Levelt, P. F., and DeCola, P.: Overview of the EOS Aura Mission, *IEEE T. Geosci. Remote*, 44, 1066–1074, 2006. 6533
- 25 Sembhi, H.: Paper in preparation, *Atmos. Meas. Tech.*, 2011. 6539
- Siddaway, J. and Petelina, S.: Transport and evolution of the 2009 Australian Black Saturday bushfire smoke in the lower stratosphere, *J. Geophys. Res.*, in press, doi:10.1029/2010JD015162, 2011. 6539
- 30 Singh, H. B., Salas, L., Herlth, D., Kolyer, R., Czech, E., Viezee, W., Li, Q., Jacob, D. J., Blake, D., Sachse, G., Harward, C. N., Fuelberg, H., Kiley, C. M., and Kondo, Y. Z. Y.: In situ measurements of HCN and CH₃CN over the pacific ocean: Sources, sinks and budgets, *J. Geophys. Res.*, 108, 8795, doi:10.1029/2002JD003006, 2003. 6535
- Teague, B., McLeod, D., and Pascoe, S.: 2009 Victorian Bushfires Royal Comission – Final

Report, Tech. rep., 2009 Victorian Bushfires Royal Commission, <http://www.royalcommission.vic.gov.au>, 2010. 6532

Waters, J. W., Froidevaux, L., Harwood, R., Jarnot, R., Pickett, H., Read, W., Siegel, P., Cofield, R., Filipiak, M., Flower, D., Holden, J., Lau, G., Livesey, N., Manney, G., Pumphrey, H., Santee, M., Wu, D., Cuddy, D., Lay, R., Loo, M., Perun, V., Schwartz, M., Stek, P., Thurstans, R., Boyles, M., Chandra, S., Chavez, M., Chen, G.-S., Chudasama, B., Dodge, R., Fuller, R., Girard, M., Jiang, J., Jiang, Y., Knosp, B., LaBelle, R., Lam, J., Lee, K., Miller, D., Oswald, J., Patel, N., Pukala, D., Quintero, O., Scaff, D., Snyder, W., Tope, M., Wagner, P., and Walch, M.: The Earth Observing System Microwave Limb Sounder (EOS MLS) on the Aura satellite, *IEEE T. Geosci. Remote Sens.*, 44, 1106–1121, 2006. 6533

Winker, D. M., Pelon, J., Jr., J. A. C., Ackerman, S. A., Charlson, R. J., Colarco, P. R., Flamant, P., Fu, Q., Hoff, R. M., Kittaka, C., Kubar, T. L., Treut, H. L., McCormick, M. P., Mégie, G., Poole, L., Powell, K., Trepte, C., Vaughan, M. A., and Wielicki, B. A.: The CALIPSO Mission: A Global 3D View of Aerosols and Clouds, *Bull. Am. Meteorol. Soc.*, 91, 1211–1229, doi:10.1175/2010BAMS3009.1, 2010. 6539

ACPD

11, 6531–6554, 2011

MLS observations of burning products

H. C. Pumphrey et al.

Title Page

Abstract

Introduction

Conclusions

References

Tables

Figures

◀

▶

◀

▶

Back

Close

Full Screen / Esc

Printer-friendly Version

Interactive Discussion



MLS observations of burning products

H. C. Pumphrey et al.

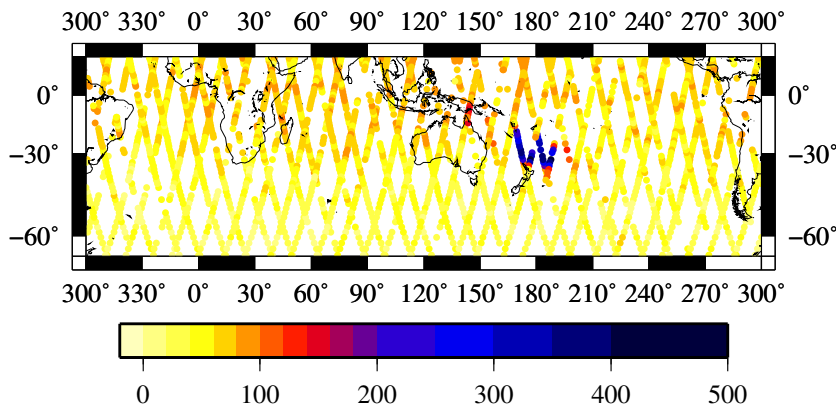


Fig. 1. MLS CO volume mixing ratio (in ppbv) at 100 hPa on 12 and 13 February 2009. Each dot represents a single MLS data point. Both descending and ascending orbits are shown. Successive ascending (or descending) orbits are separated by 24° of longitude. The ascending orbit tracks for a given day are displaced by approximately 12° of longitude from those of the previous day. Values plotted as purple and blue are much larger than those usually seen at this altitude. Negative values occur in places where the mixing ratio is small compared to the measurement error.

[Title Page](#)
[Abstract](#)
[Introduction](#)
[Conclusions](#)
[References](#)
[Tables](#)
[Figures](#)
[◀](#)
[▶](#)
[◀](#)
[▶](#)
[Back](#)
[Close](#)
[Full Screen / Esc](#)
[Printer-friendly Version](#)
[Interactive Discussion](#)


MLS observations of
burning products

H. C. Pumphrey et al.

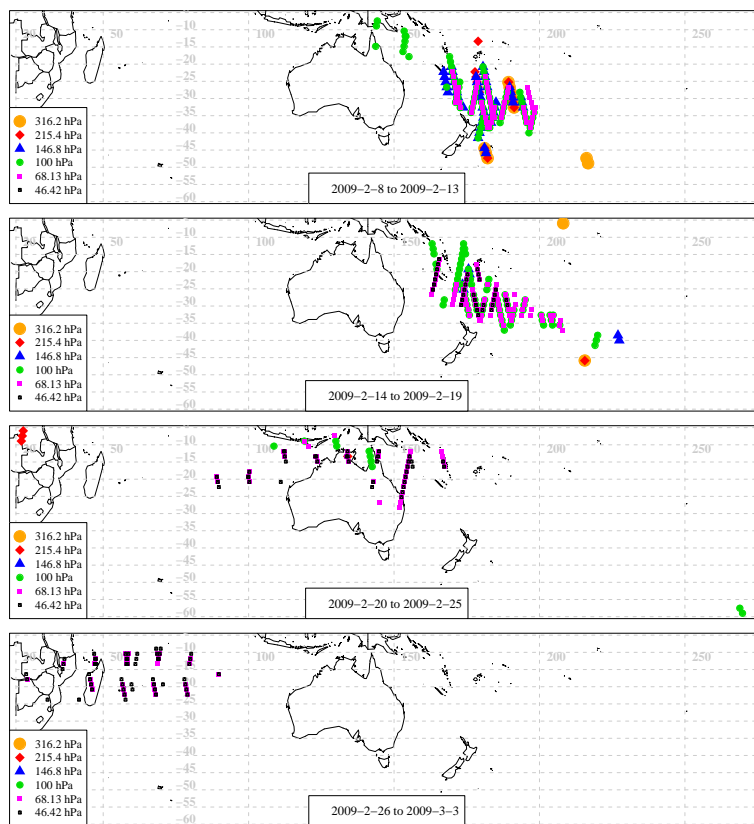


Fig. 2. Locations of MLS measurements where the CO values are anomalously high as defined in the text. The four maps show four successive 6-day periods beginning on 8 February, one day after the Black Saturday fire. (Dates are shown at the bottom of each panel in the form Year-month-day.) Apart from a few instances at the higher pressures, these points all appear to be part of the same event.

Title Page

Abstract

Introduction

Conclusions

References

Tables

Figures

◀

▶

◀

▶

Back

Close

Full Screen / Esc

Printer-friendly Version

Interactive Discussion



MLS observations of
burning products

H. C. Pumphrey et al.

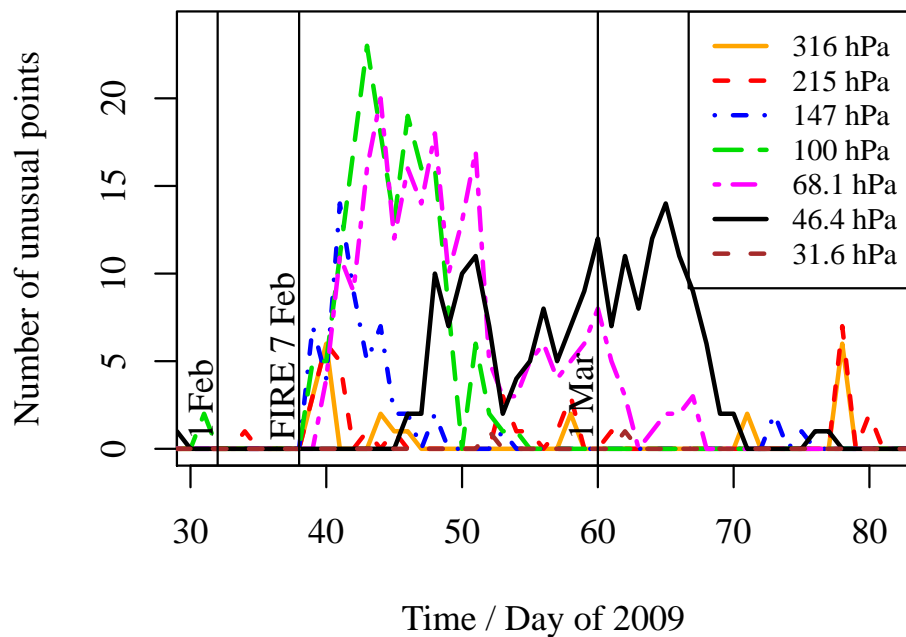


Fig. 3. Number of points for each day for which the CO mixing ratio was identified as unusual (as defined in the text) in the 5° S–60° S latitude range.

[Title Page](#)[Abstract](#)[Introduction](#)[Conclusions](#)[References](#)[Tables](#)[Figures](#)[◀](#)[▶](#)[◀](#)[▶](#)[Back](#)[Close](#)[Full Screen / Esc](#)[Printer-friendly Version](#)[Interactive Discussion](#)

MLS observations of
burning products

H. C. Pumphrey et al.

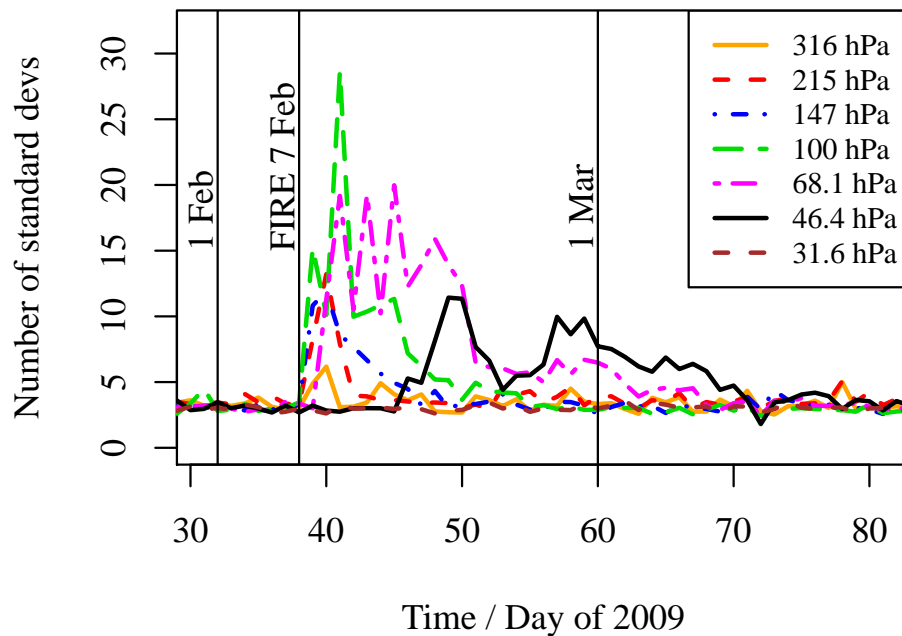


Fig. 4. Mean number of standard deviations above the mean CO mixing ratio for the points identified as unusual in Fig. 3.

[Title Page](#)[Abstract](#)[Introduction](#)[Conclusions](#)[References](#)[Tables](#)[Figures](#)[◀](#)[▶](#)[◀](#)[▶](#)[Back](#)[Close](#)[Full Screen / Esc](#)[Printer-friendly Version](#)[Interactive Discussion](#)

MLS observations of
burning products

H. C. Pumphrey et al.

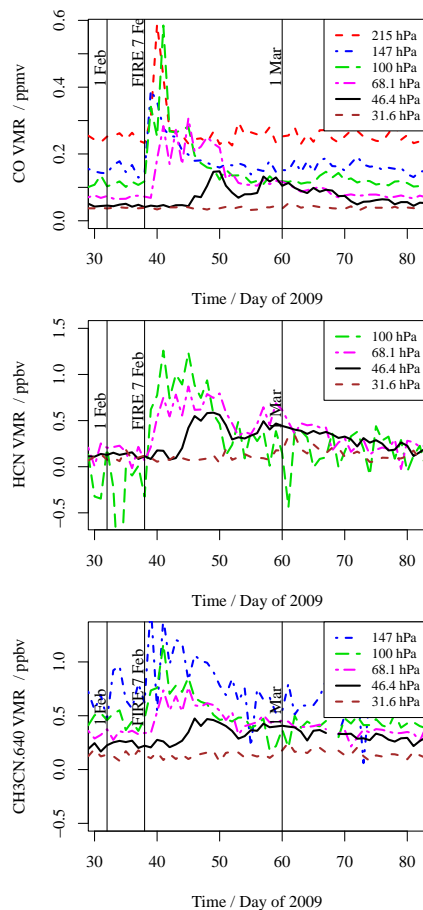


Fig. 5. Time series of the mixing ratio of MLS CO, HCN and CH₃CN within the polluted airmass. The CH₃CN shown is that derived from the 640 GHz measurements.

Title Page

Abstract

Introduction

Conclusions

References

Tables

Figures

◀

▶

◀

▶

Back

Close

Full Screen / Esc

Printer-friendly Version

Interactive Discussion



**MLS observations of
burning products**

H. C. Pumphrey et al.

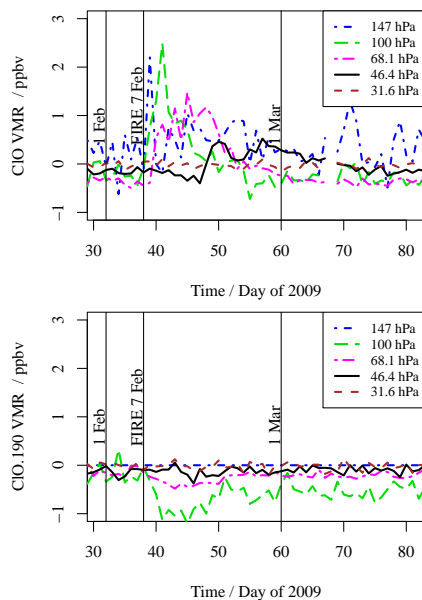


Fig. 6. Time series of the mixing ratio of MLS CIO within the polluted airmass.

[Title Page](#)[Abstract](#)[Introduction](#)[Conclusions](#)[References](#)[Tables](#)[Figures](#)[◀](#)[▶](#)[◀](#)[▶](#)[Back](#)[Close](#)[Full Screen / Esc](#)[Printer-friendly Version](#)[Interactive Discussion](#)

MLS observations of
burning products

H. C. Pumphrey et al.

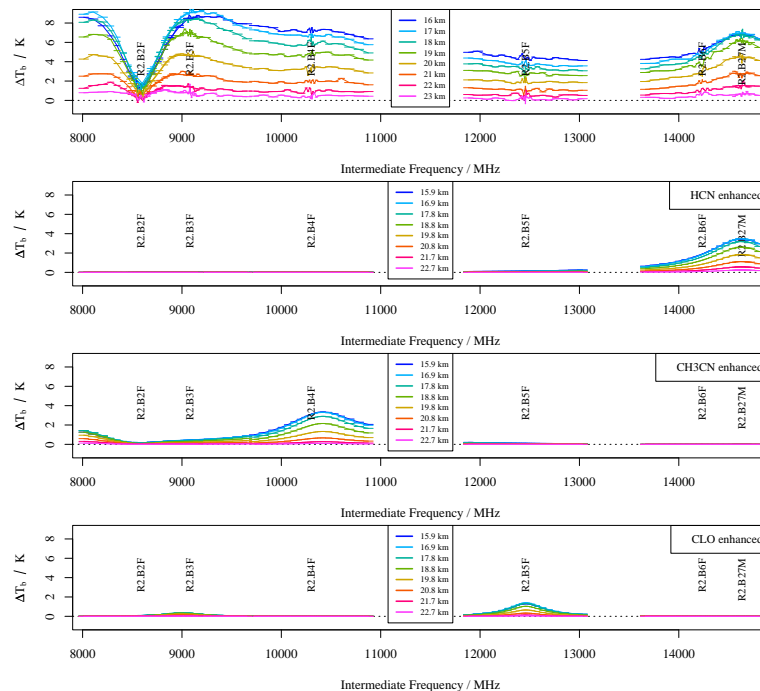


Fig. 7. Some spectra from the 190 GHz radiometer (R2) of MLS. The top panel is the measured difference between spectra in the plume and out of it. The other three panels show the difference between a default calculated spectrum and ones for which HCN, CH₃CN and ClO are enhanced by roughly the amount observed in the retrieved profiles. If the top panel shows features similar to those in one of the other panels, this implies that the species which is enhanced in the calculation for the lower panel was also enhanced in the plume region. The vertical labels (e.g. R2.B5F) mark the centres of the individual filterbanks or “bands” which analyse the signal from this radiometer.

Title Page

Abstract

Introduction

Conclusions

References

Tables

Figures

◀

▶

◀

▶

Back

Close

Full Screen / Esc

Printer-friendly Version

Interactive Discussion



MLS observations of
burning products

H. C. Pumphrey et al.

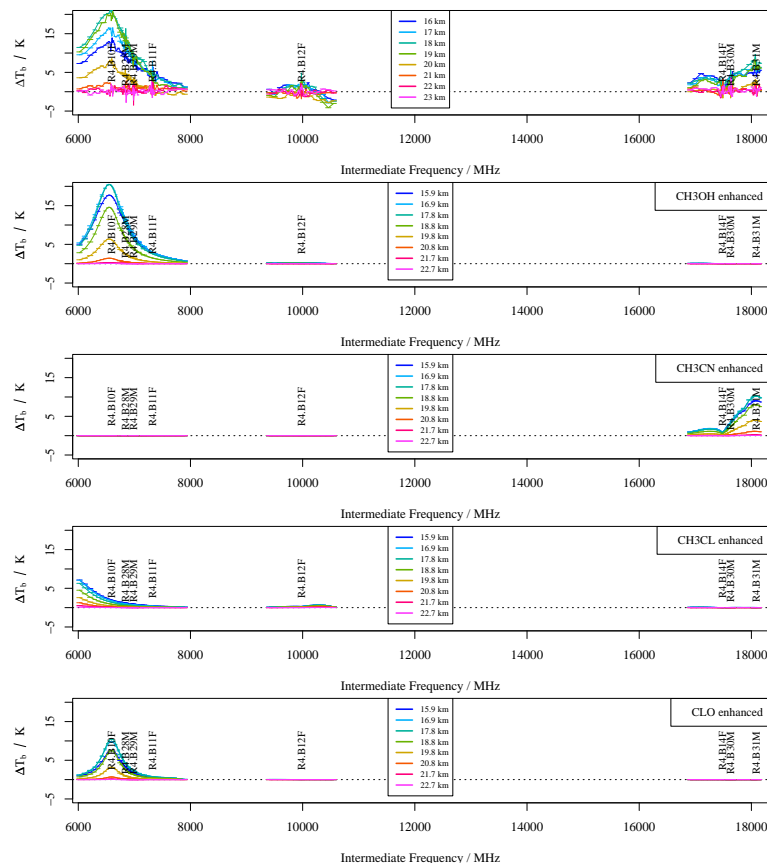


Fig. 8. Some spectra from the 640 GHz radiometer (R4) of MLS, plotted in the same manner as in Fig. 7. The top panel is the measured difference between spectra in the plume and out of it. The other four panels show the difference between a default calculated spectrum and ones for which CH_3OH , CH_3CN , CH_3Cl and ClO are enhanced by roughly the amount observed in the retrieved profiles.

Title Page

Abstract

Introduction

Conclusions

References

Tables

Figures

◀

▶

◀

▶

Back

Close

Full Screen / Esc

Printer-friendly Version

Interactive Discussion



MLS observations of
burning products

H. C. Pumphrey et al.

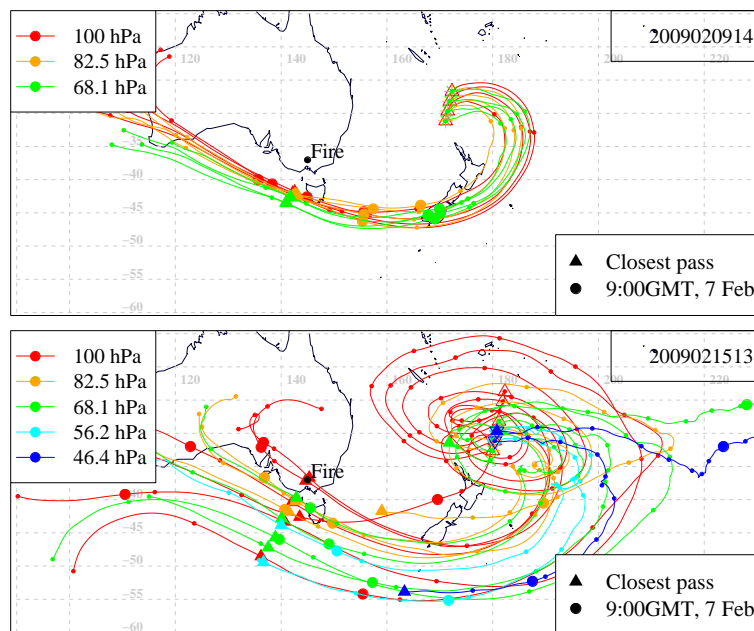


Fig. 9. Examples of back trajectories run from MLS measurement locations with elevated CO levels. The measurements in the top panel were made within 30 min of 14:00 on 9 February, while those in the bottom panel were made within 30 min of 13:00 on 15 February. (Starting date and hour is shown on each panel in the form YYYYMMDDHH.) The small dots on the trajectories are placed at 24-h intervals.

Title Page

Abstract

Introduction

Conclusions

References

Tables

Figures

◀

▶

◀

▶

Back

Close

Full Screen / Esc

Printer-friendly Version

Interactive Discussion



MLS observations of
burning products

H. C. Pumphrey et al.

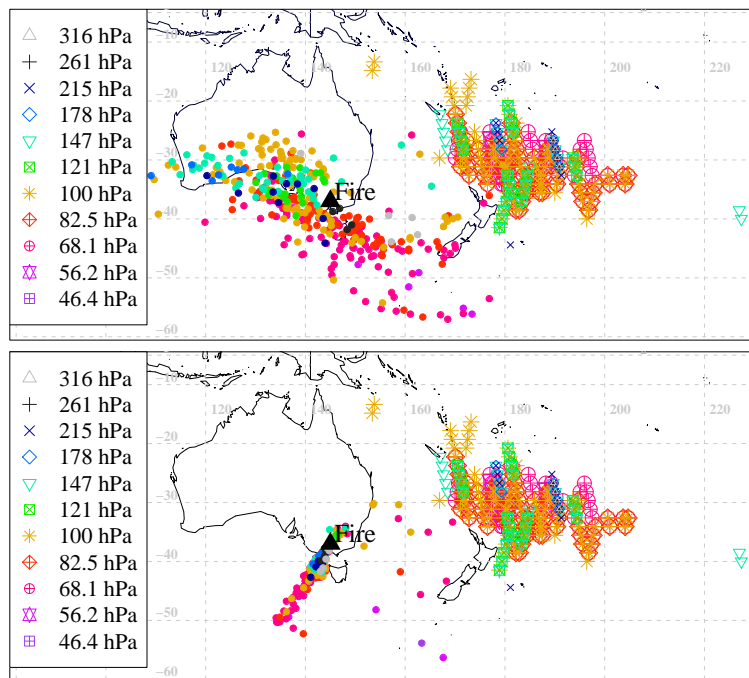


Fig. 10. Back trajectories run from MLS measurement locations with elevated CO levels for the ten days after the fire. The symbols in the legend show the locations of the MLS measurements. The filled circles show the trajectory location at 09:00 on 7 February (upper map: examples are shown as filled circles in Fig. 9) and at the time of their closest pass to the fire region (lower map: examples are shown as triangles in Fig. 9).

Title Page

Abstract

Introduction

Conclusions

References

Tables

Figures

◀

▶

◀

▶

Back

Close

Full Screen / Esc

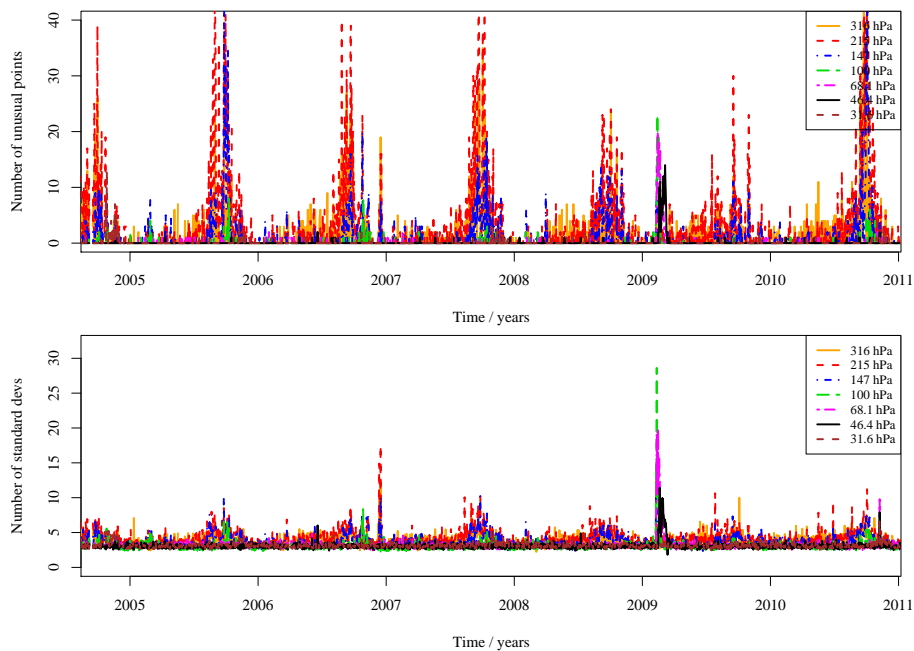
Printer-friendly Version

Interactive Discussion



**MLS observations of
burning products**

H. C. Pumphrey et al.

**Fig. 11.** As per Figs. 3 and 4 but for the whole mission.[Title Page](#)[Abstract](#)[Introduction](#)[Conclusions](#)[References](#)[Tables](#)[Figures](#)[◀](#)[▶](#)[◀](#)[▶](#)[Back](#)[Close](#)[Full Screen / Esc](#)[Printer-friendly Version](#)[Interactive Discussion](#)